

INFLUENCE OF DOPING ON THE LATTICE DYNAMICS OF GALLIUM NITRIDE

A. Kaschner, H. Siegle*, A. Hoffmann, C. Thomsen

Institut für Festkörperphysik, Technische Universität Berlin, Hardenbergstraße 36, 10623 Berlin, Germany

*Present address: Lawrence Berkeley National Laboratory, Berkeley, California 94720, USA

U. Birkle, S. Einfeldt, D. Hommel

Institut für Festkörperphysik, FB 1, Univ. Bremen, Kufsteiner Str. NW 1, 28359 Bremen, Germany

Cite this article as: MRS Internet J. Nitride Semicond. Res. 4S1, G3.57 (1999)

Abstract

We present results of Raman-scattering experiments on GaN doped with Si, C, and Mg, respectively, grown by molecular beam epitaxy (MBE). The influence of the different dopants on strain and free-carrier concentration was investigated. Furthermore, we report on several local vibrational modes (LVM) around 2200 cm^{-1} in Raman spectra of highly Mg-doped GaN. A possible explanation of these high-energy modes in terms of hydrogen-related vibrations is given. We also found a variety of new structures in the range of the GaN host lattice phonons. Secondary ion mass spectroscopy (SIMS) was applied to determine the concentration of magnesium and unintentionally incorporated hydrogen.

Introduction

Much attention has been paid to the wide-bandgap material GaN due to its high potential for optoelectronic and high-power electronic applications [1]. Controlled p- and n-doping is a major issue for the fabrication of electronic devices based on group III-Nitrides. The growth of doped GaN epilayers and heterostructures by molecular beam epitaxy offers the advantage of lower unintentional dopant concentration in the material. Among the optical properties of doped GaN the influence of doping on the lattice dynamics is of special interest. Raman-spectroscopy is a powerful tool to investigate the correlation between doping, strain [2], and free-carrier concentration [3].

Moreover, dopant atoms can give rise to local vibrational modes (LVM) due to their different masses compared with those of the substituted elements [4]. High-energy modes are reported for Mg-doped GaN [5, 6] which were assumed to be related to hydrogen complexes. This is of special interest, because hydrogen is known as a compensating center for magnesium acceptors. To our knowledge, no LVM for Si-, C-, or Mg-doped GaN in the range of the host lattice phonons have been reported in literature so far.

Experiment

The Raman-scattering experiments were carried out in backscattering geometry with a triple-grating spectrometer equipped with a cooled charge-coupled device detector. The 488 nm line of an Ar^+/Kr^+ mixed-gas laser was used for excitation. The Raman shifts were determined with an accuracy better than 1 cm^{-1} . Microscope optics allowed spatially-resolved measurements with a resolution of about $0.7\text{ }\mu\text{m}$.

The samples under study were Si-, C-, and Mg-doped GaN films of about 1 μm thickness grown on sapphire (0001) substrates by MBE; the details are given elsewhere [7]. The Mg-doped samples A and B were p-conductive with a hole concentration at room temperature of $3.7 \cdot 10^{17} \text{ cm}^{-3}$ and $1.4 \cdot 10^{17} \text{ cm}^{-3}$, respectively, whereas the other two samples were compensated but n-conductive. Secondary ion mass spectroscopy was applied to determine the concentration of magnesium and hydrogen. The measured concentrations are accurate to within 20% deviation. The dopant concentration of the Si- and C-doped GaN films were estimated in terms of growth conditions. The free-electron concentration in the Si-doped samples varied from $8.1 \cdot 10^{15} \text{ cm}^{-3}$ to $1.3 \cdot 10^{20} \text{ cm}^{-3}$ as determined by Hall measurements.

Results

1. Local vibrational modes in doped GaN

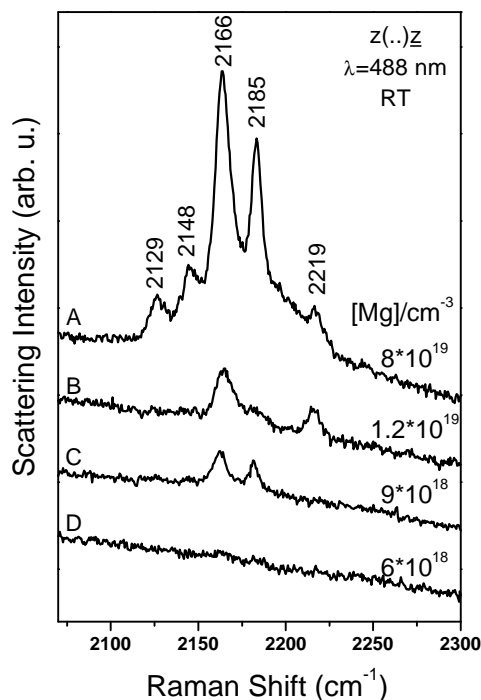


Figure 1: Room-temperature Raman spectra of GaN with different magnesium content in the high-energy range.

Figure 1 shows Raman spectra of samples with the respective magnesium concentrations of $8 \cdot 10^{19} \text{ cm}^{-3}$ (A), $1.2 \cdot 10^{19} \text{ cm}^{-3}$ (B), $9 \cdot 10^{18} \text{ cm}^{-3}$ (C) and $6 \cdot 10^{18} \text{ cm}^{-3}$ (D) in the high-energy region. In the spectrum of sample A with the highest magnesium concentration a new mode appears at 2129 cm^{-1} in addition to the four LVM described in Ref. 5. Apparently, the intensity of the modes correlates with the magnesium content. A Mg-concentration of around $1 \cdot 10^{19} \text{ cm}^{-3}$ is necessary for some of the high-energy modes to appear well-resolved in the spectra. The hydrogen concentration for all the samples investigated is about $1 \cdot 10^{19} \text{ cm}^{-3}$ as determined by secondary ion mass spectroscopy. Since hydrogen was not intentionally supplied during growth its incorporation possibly arises from the residual water vapor pressure in the growth chamber.

Yi et al. [8] observed a similar structure of five modes around 2800 cm^{-1} in Mg-doped GaN grown by metalorganic vapor phase epitaxy (MOVPE). These modes were attributed to symmetric and asymmetric C-H_n ($n=1, 2, 3$) vibrations due to carbon incorporation caused by the decomposition of the magnesium precursor during growth. Remarkably, the frequency ratio for all the five modes is between 1.33 and 1.34. This is close to $\sqrt{2}$, a value expected for similar vibrations with carbon ($m_{\text{C}}=12.01 \text{ u}$) replaced by magnesium ($m_{\text{Mg}}=24.31 \text{ u}$). This implies that magnesium is built into the lattice on a nitrogen site with force constants similar to those of carbon, an interpretation which seems doubtful. Furthermore, there are experimental and theoretical articles that determined the frequency of the Mg-H vibration above 3000 cm^{-1} [5, 9].

Alternatively, hydrogen-decorated native defects or hydrogen at extended defects such as dislocations can give rise to high-energetic vibrations. When the Fermi level reaches a value below 2.1 eV the formation of $\text{V}_{\text{Ga}}\text{-H}_n$ complexes with $n=1, 2, 3$ is likely to occur with a predicted frequency of 3100 cm^{-1} for a $\text{V}_{\text{Ga}}\text{-H}$ complex [10]. This is much higher than the frequencies we observe, even if anharmonic terms may lower the frequency considerably [10].

However, we rather believe that the magnesium incorporation causes the high-energy modes indirectly by creating defects or by lowering the Fermi level and therefore making the the hydrogen complex formation likely [11].

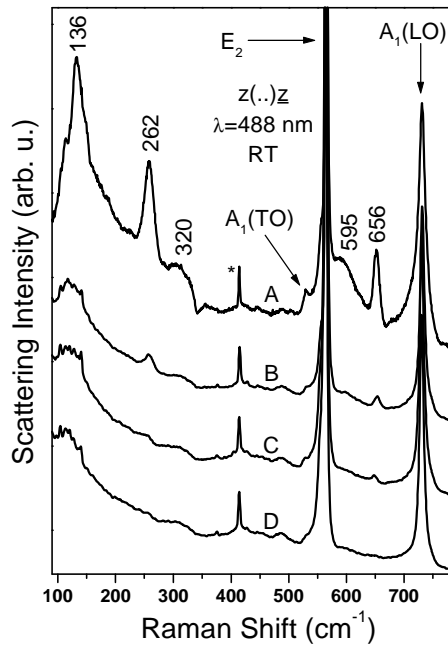


Figure 2: Room-temperature Raman spectra (normalized to E_2 intensity) of GaN with different magnesium content in the low-energy range. Apart from the host lattice phonons five additional modes are observed. The peak marked by an asterisk is a phonon from the sapphire substrate.

Apart from the five high-energy modes the highly Mg-doped samples exhibit new vibrational modes in the region of the acoustic and optical GaN phonons. We found structures at 136 cm^{-1} , 262 cm^{-1} , 320 cm^{-1} , 595 cm^{-1} and 656 cm^{-1} . Figure 2 displays the low-energy part of the Raman spectra of the four samples in the same sequence as in Figure 1. The broad structures centered around 320 cm^{-1} and 595 cm^{-1} may result from disorder-activated scattering, in which built-in defects yield a relaxation of the $q=0$ selection rule for first-order Raman scattering. This interpretation is supported by the fact that from sample D to A the forbidden $A_1(\text{TO})$ mode at 533 cm^{-1} increases considerably in intensity. Limmer et al. [12] reported on a disorder-activated Raman-mode around 300 cm^{-1} in ion-implanted GaN which is close to our 320 cm^{-1} mode. Furthermore, the cut-off at 340 cm^{-1} fits well with calculated phonon dispersion curves [13, 14]. On the other hand, the modes at 136 cm^{-1} , 262 cm^{-1} and 656 cm^{-1} probably do not originate from disorder-activated scattering since the phonon density of states (PDOS) does not exhibit marked structures in this frequency range [14]. Recently, a mode at 656 cm^{-1} was observed in GaN after annealing at 1000°C and related to a damaged-sapphire substrate [15]. The mode we

observed at 656 cm^{-1} is of different origin since it does not scale with the intensity of the sapphire mode at 418 cm^{-1} nor with other modes of the damaged-sapphire at e.g. 770 cm^{-1} but rather with the Mg-concentration.

We thus believe these structures in the low-energy range to be correlated with magnesium. Equation (1) gives us a rough estimate of the magnesium local vibrational mode frequency from the effective masses of the GaN and LVM vibrations.

$$\frac{\omega_{\text{GaN}}}{\omega_{\text{LVM}}} \approx \sqrt{\frac{\mu_{\text{LVM}}}{\mu_{\text{GaN}}}} \quad (1)$$

Assuming that magnesium occupies a gallium site we obtain a value of about 640 cm^{-1} for N-Mg vibrations using $\omega_{\text{GaN}} = \omega(E_1(\text{TO})) = 560\text{ cm}^{-1}$.

Though the 656 cm^{-1} mode lies in the range of the optical phonons its observation may be possible because the PDOS is relatively low in the region from 640 cm^{-1} to 675 cm^{-1} as confirmed by second-order Raman-scattering [13] and time-of-flight neutron spectroscopy [14]. We hence assign the 656 cm^{-1} mode to a local vibrational mode of magnesium in GaN. The Mg-concentration in the 10^{19} cm^{-3} range is apparently sufficient to observe the LVM without resonant excitation.

The nature of the 136 cm^{-1} and 262 cm^{-1} mode remains unclear. Since the density of states is also relatively low in the energy range of the two modes in question it is conceivable that they are also LVM.

We did not observe any LVM for the Si- and C-doped GaN samples in low-energy range nor in the high-energy range.

2. Biaxial Stress due to incorporation of dopants

Due to its nonpolar character the E_2 phonon frequency is a good measure for biaxial stress in GaN layers. Biaxial compressive stress increases the phonon frequency. Values of $4.2 \text{ cm}^{-1}/\text{GPa}$ [2], $6.2 \text{ cm}^{-1}/\text{GPa}$ [16] and $7.7 \text{ cm}^{-1}/\text{GPa}$ [17] have been reported. Figure 3 shows the dependence of the E_2 frequency on the dopant concentration. While the E_2 values remain nearly constant between 567 cm^{-1} and 568 cm^{-1} over the whole doping range in case of the silicon doping series, we see a strong hardening in the magnesium series for Mg-concentrations exceeding $1 \cdot 10^{19} \text{ cm}^{-3}$. This

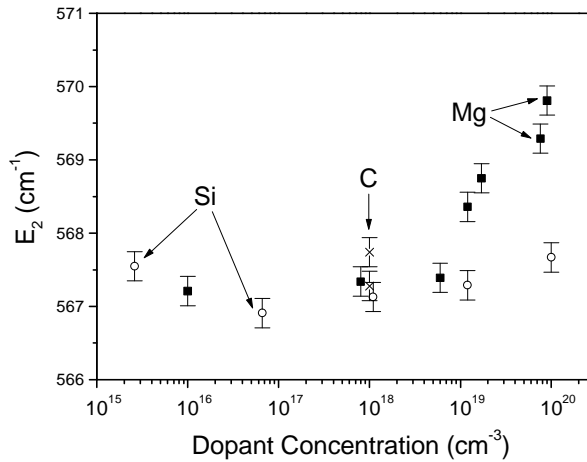


Figure 3: Position of the E_2 mode for different doped GaN samples.

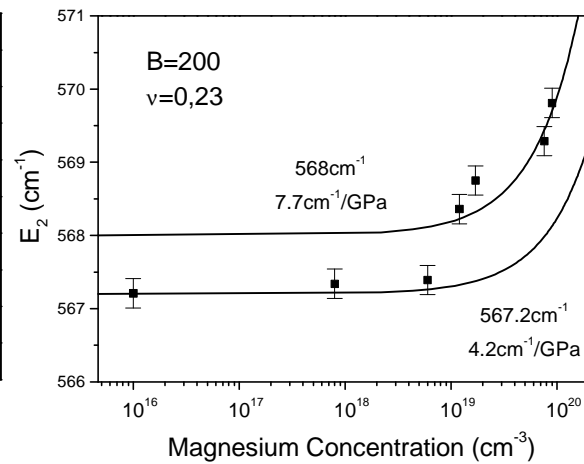


Figure 4: E_2 position vs. Mg-concentration. The lines show the predicted behavior using eq. (2) and (3) with different values for the bulk E_2 frequency and the E_2 shift. The values for B and ν are taken from Ref. 2.

behavior can be explained by the different size of the dopant atom ($r_{\text{Mg}}=0.14 \text{ nm}$) and the replaced host atom ($r_{\text{Ga}}=0.126 \text{ nm}$). Using equation (2) one can calculate the influence of this effect on the strain [2].

$$\varepsilon = \frac{c - c_0}{c_0} = \frac{\left[1 - \left(\frac{r_{\text{Mg}}}{r_{\text{Ga}}} \right)^3 \right] \cdot C}{3N} \quad (2)$$

Here, N is the number of lattice sites of the host matrix, C the dopant concentration, c and c_0 the strained and unstrained lattice constant, respectively. Equation (3), where B is the bulk modulus and ν is the Poisson ratio, correlates the strain with the biaxial stress.

$$\sigma = \varepsilon \cdot \frac{B}{\nu} \quad (3)$$

Figure 4 shows the experimental data of the Mg-doped samples and calculated curves with different values for the strain-free E_2 frequency and $\Delta\omega(E_2)/\Delta\sigma$. It is obvious that the observed behavior can be explained by a size effect qualitatively, but the uncertainty for the basic GaN material parameters renders exact calculations difficult.

When substituting gallium by silicon one would expect the same effect but with opposite sign since the atomic radius of silicon is smaller than that of gallium. Surprisingly, we did not observe any significant shift for the E_2 frequency up to a silicon concentration of $1 \cdot 10^{20} \text{ cm}^{-3}$. The highly Si-doped samples do also exhibit a large free-carrier concentration (see next chapter). Therefore we believe,

that the size effect is compensated by the change of the lattice constant due to free electrons [17]. Following Ref. 18 a free-carrier concentration of $5 \cdot 10^{19} \text{ cm}^{-3}$ should increase the lattice constant by 0.01% which equals the absolute value of the size effect caused by the same silicon concentration. The carbon concentration of the samples in our study is too low to observe a significant E_2 shift.

3. Determination of the free-carrier concentration

The interaction of free charge carriers with longitudinal optical phonons leads to the observation of longitudinal phonon plasmon modes (LPP) [3]. If damping can be neglected the frequency of the LPP modes is given by equation (4).

$$(\omega_{\text{LPP}}^{\pm})^2 = 0.5 \cdot \left\{ \omega_{\text{L}}^2 + \omega_{\text{P}}^2 \pm \left[(\omega_{\text{L}}^2 + \omega_{\text{P}}^2)^2 - 4\omega_{\text{P}}^2\omega_{\text{T}}^2 \right]^{1/2} \right\} \quad (4)$$

Here, ω_{L} and ω_{T} are the frequencies of the LO and TO phonons, respectively. The plasmon frequency is correlated with the free-carrier concentration.

$$\omega_{\text{P}}^2 = \frac{ne^2}{m^* \epsilon_{\infty} \epsilon_0} \quad (5)$$

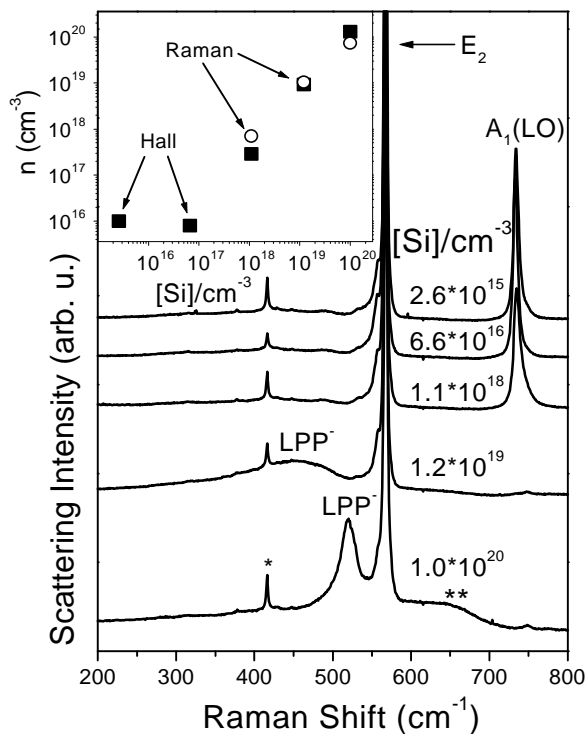


Figure 5: Room-temperature Raman spectra of different Si-doped samples. The inset shows the carrier concentration determined by Hall and Raman measurements vs. Si-content.

In equation (5) n and m^* are the concentration and effective mass of the charge carriers, ϵ_{∞} the high-frequency dielectric constant.

In Figure 5 the spectra of five samples with silicon concentrations between $2.6 \cdot 10^{15} \text{ cm}^{-3}$ (top) and $1.0 \cdot 10^{20} \text{ cm}^{-3}$ (bottom) are plotted. The two highest doped samples exhibit LPP⁻ modes at 450 cm^{-1} and 520 cm^{-1} . The $A_1(\text{LO})$ mode already vanished and therefore the LPP⁺ mode appears at 2580 cm^{-1} and 1070 cm^{-1} (not shown). From equations (4) and (5) we calculated the corresponding carrier concentration to be $7.4 \cdot 10^{19} \text{ cm}^{-3}$ and $1.0 \cdot 10^{19} \text{ cm}^{-3}$, respectively. Notice that in both spectra a structure at around 650 cm^{-1} (***) appears which is only known from highly doped GaN [19]. The $A_1(\text{LO})$ mode of the sample with a silicon concentration of about $1.1 \cdot 10^{18} \text{ cm}^{-3}$ appears slightly asymmetric typical for carrier concentrations between $5 \cdot 10^{17} \text{ cm}^{-3}$ and $1 \cdot 10^{18} \text{ cm}^{-3}$. For the remaining two samples the free-carrier concentration is too low to cause any shift or broadening of the $A_1(\text{LO})$ mode and cannot be determined by this method. The inset of Figure 5 compares the free-carrier concentration determined by Hall measurements

and by Raman spectroscopy as a function of the silicon concentration. Both data sets agree well. Raman spectroscopy offers the advantage that the free-carrier concentration can be determined with a spatial resolution better than $1 \mu\text{m}$ without contacting the samples.

Conclusions

In this work we have shown that a variety of information about doped GaN crystals can be obtained by Raman spectroscopy. We found LVM of magnesium in the region of the host lattice phonons as well as in the high-energy range which now may serve as an indicator for the incorporation of magnesium. No LVM were observed for our Si- and C-doped GaN samples. Doping with atoms of a different size than the substituted host atom causes internal stress which can be obtained via the shift of the nonpolar E_2 mode. For Mg-doped samples we found that the biaxial stress increases with dopant concentration while in case of silicon the size effect is roughly compensated by the increasing free-carrier concentration. The free carrier concentration of doped GaN can be determined by the frequency of the LPP modes.

Acknowledgment

We thank W. Kriegseis (University of Gießen) and M. Straßburg (TU Berlin) for carrying out the SIMS measurements. A.K. acknowledges the support of an Ernst von Siemens scholarship and H.S. a DAAD fellowship.

References

- [1] See for example, S. N. Mohammad, A. Salvador, and H. Morkoç, *Proc. of the IEEE* **83**, 1306 (1995).
- [2] C. Kisielowski, J. Krüger, S. Ruvimov, T. Suski, J. W. Ager III, E. Jones, Z. Lilienthal-Weber, M. Rubin, E. R. Weber, M. D. Bremser, and R. F. Davis, *Phys. Rev. B* **54**, 17745 (1996).
- [3] P. Perlin, J. Camassel, W. Knap, T. Taliercio, J. C. Chervin, T. Suski, I. Grzegory, S. Porowski, *Appl. Phys. Lett.* **67**, 2524 (1995).
- [4] A. S. Barker, Jr. and A. J. Sievers, *Rev. Mod. Phys.* **47**, Suppl. 2, S1 (1975).
- [5] M. S. Brandt, J. W. Ager III, W. Götz, N. M. Johnson, J. S. Harris, R. J. Molnar, and T. D. Moustakas, *Phys. Rev. B* **49**, R14758, (1994).
- [6] W. Götz, N. M. Johnson, D. P. Bour, M. D. McCluskey, and E. E. Haller, *Appl. Phys. Lett.* **69**, 3725 (1996).
- [7] S. Einfeldt, U. Birkle, C. Thomas, M. Fehrer, H. Heinke, and D. Hommel, *Mat. Sci. Eng. B* **50**, 12 (1997).
- [8] G.-C. Yi and B. W. Wessels, *Appl. Phys. Lett.* **70**, 357 (1997).
- [9] J. Neugebauer and C. G. van de Walle, *Phys. Rev. Lett.* **75**, 4452 (1995).
- [10] C. G. van de Walle, *Phys. Rev. B* **56**, R10020 (1997).
- [11] A. Kaschner, H. Siegle, M. Straßburg, A. Hoffmann, C. Thomsen, U. Birkle, S. Einfeldt, and D. Hommel: "Low-energy lattice vibrations in Mg-doped GaN grown by MBE", submitted to *Appl. Phys. Lett.*
- [12] W. Limmer, W. Ritter, R. Sauer, B. Mensching, C. Liu, and B. Rauschenbach, *Appl. Phys. Lett.* **72**, 2589 (1998).
- [13] H. Siegle, G. Kaczmarczyk, L. Filippidis, A. P. Litvinchuk, A. Hoffmann, and C. Thomsen, *Phys. Rev. B* **55**, 7000 (1997).
- [14] J. C. Nipko, C.-K. Loong, C. M. Balkas and R. F. Davis, *Appl. Phys. Lett.* **73**, 34 (1998).
- [15] M. Kuball, F. Demangeot, J. Frandon, M. A. Renucci, J. Massies, N. Grandjean, R. L. Aulombard, and O. Briot, *Appl. Phys. Lett.* **73**, 960 (1998).
- [16] T. Kozawa, T. Kachi, H. Kano, H. Nagase, N. Koide, and K. Manabe, *J. Appl. Phys.* **77**, 4389 (1995).
- [17] I.-H. Lee, I.-H. Choi, C.-R. Lee, E.-J. Shin, D. Kim, S. K. Noh, S.-J. Son, K. Y. Lim, and H. J. Lee, *J. Appl. Phys.* **83**, 5787 (1998).
- [18] M. Leszczynski, H. Teisseyre, T. Suski, I. Grzegory, M. Bockowski, J. Jun, S. Porowski, K. Pakula, J. M. Baranowski, C. T. Foxon, T. S. Cheng, *Appl. Phys. Lett.* **69**, 73 (1996).
- [19] F. Demangeot, J. Frandon, M. A. Renucci, C. Meny, O. Briot, and R. L. Aloumbard, *J. Appl. Phys.* **82**, 1305 (1997).